

# Cylindrical Resonator Sectorally Filled with DNG Metamaterial and Excited by a Line Source

Vito G. Daniele, Roberto D. Graglia, *Fellow, IEEE*, Guido Lombardi, *Senior Member, IEEE*,  
and Piergiorgio L. E. Uslenghi, *Life Fellow, IEEE*

**Abstract**—A circular cylindrical resonator with metallic walls is analyzed, in the phasor domain. The resonator contains a wedge of DNG metamaterial that is anti-isorefractive to the DPS material filling the remaining volume of the resonator, and whose edge is located on the resonator axis. The resonance conditions are established. The problem of an electric line source parallel to the axis and located anywhere inside the DPS region is solved exactly. Numerical results are presented and discussed.

**Index Terms**—Cavity resonator, electromagnetic theory, metamaterial.

## I. INTRODUCTION

THE idea of using double-negative (DNG) metamaterial inside cavities to build resonators was introduced by Engheta [1]-[2], who proposed a one-dimensional resonator containing double-negative (DNG) metamaterial in part of its volume. By utilizing phase compensation between the double-positive (DPS) and DNG portions of the structure, it is possible to build resonators that perform independently of dimensions, at the frequencies for which the DNG metamaterial behaves as postulated. Subsequently, this concept was extended to fully three-dimensional cavity resonators by Couture et al. [3]-[4] and by Uslenghi [5]-[6]. A review of these structures was presented in [7].

In this paper, a circular cylindrical resonator with metallic (PEC) walls sectorally filled in part with double-positive (DPS) material and in part with double-negative (DNG) metamaterial is considered. The boundaries separating the DPS and DNG regions are the faces of a wedge of arbitrary aperture angle, whose edge coincides with the axis of the resonator. The DPS region is filled with a linear, uniform and isotropic material characterized by a real positive electric permittivity  $\varepsilon$  and a real positive magnetic permeability  $\mu$ , or alternatively by a real positive wavenumber  $k = \omega\sqrt{\varepsilon\mu}$  and a real positive intrinsic impedance  $Z = \sqrt{\mu/\varepsilon}$ , where  $\omega$  is the angular frequency. The DNG region is filled with a linear, uniform and isotropic material characterized by a real negative permittivity  $-\varepsilon$  and a real negative permeability  $-\mu$ , or alternatively by a real negative wavenumber  $-k$  and a real positive intrinsic impedance  $Z$ . Thus, the DPS and DNG regions of

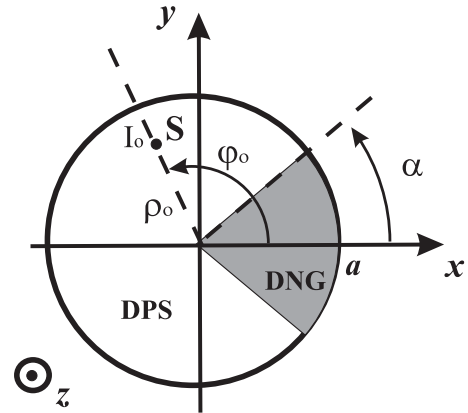


Fig. 1. Cross section of the resonator

the resonator are filled with materials having real refractive indexes of opposite sign and the same real intrinsic impedance. The analysis is conducted in the phasor domain with time-dependence factor  $e^{+j\omega t}$ . The results obtained are valid at those frequencies where the DNG metamaterial behaves as postulated. Because of the dispersive properties of passive DNG materials, broadbanding may be achievable only by the use of active (non-Foster) metamaterials. Preliminary analyses of this problem were orally presented by the authors of this paper at two symposia [8]-[9]. The geometry of the problem and the condition that must be satisfied for resonance to occur are described in Section II. Excitation by an electric line source parallel to the axis of the cylinder and located anywhere inside the DPS volume is considered; this problem is solved analytically in Section III, and some numerical results based on this exact solution are shown and discussed in Section IV.

## II. GEOMETRY OF THE PROBLEM AND RESONANCE CONDITION

A cross section of the resonator in a plane perpendicular to its axis is shown in Fig. 1.

The cylinder has a metallic (PEC) boundary, radius  $a$ , and length  $d$ . Since we limit our considerations to electric fields parallel to the axis  $z$  of the resonator, the boundary-value problem is two-dimensional and, the  $z$  coordinate and the length  $d$  do not play any role in our analysis. With reference to cylindrical coordinates  $(\rho, \varphi, z)$ , the DPS material occupies the cross sectional area  $(0 \leq \rho \leq a, \alpha \leq \varphi \leq 2\pi - \alpha)$ , whereas the DNG material occupies the area  $(0 \leq \rho \leq a, -\alpha \leq \varphi \leq \alpha)$ . The semi-aperture angle  $\alpha$  of the DNG wedge may vary over the interval  $0 \leq \varphi \leq \pi$ , where  $\alpha = 0$  if the

V.G. Daniele is with Dipartimento di Elettronica e Telecomunicazioni, Politecnico di Torino, 10129 Torino, Italy e-mail: vito.daniele@polito.it.

R.D. Graglia and G. Lombardi are with Dipartimento di Elettronica e Telecomunicazioni, Politecnico di Torino, 10129 Torino, Italy e-mails: roberto.graglia@polito.it, guido.lombardi@polito.it.

P.L.E. Uslenghi is with the Department of Electrical and Computer Engineering and the Department of Physics, University of Illinois at Chicago, Illinois 60607, USA e-mail: uslenghi@uic.edu.

Manuscript received June 30, 2012.

resonator is entirely filled with DPS material, and  $\alpha = \pi$  if it is filled with DNG material.

The electric field inside the resonator is assumed to be of the form:

$$\mathbf{E}^\pm = \hat{z}E_z^\pm(\rho, \varphi) = \hat{z}J_\nu(\pm k\rho)[A_\nu^\pm \sin(\nu\varphi) + B_\nu^\pm \cos(\nu\varphi)] \quad (1)$$

where the upper (lower) sign applies to the DPS (DNG) sub-volume. Consequently, the magnetic field components are

$$H_\rho^\pm(\rho, \varphi) = \frac{\pm j\nu}{\omega\mu\rho} J_\nu(\pm k\rho)[A_\nu^\pm \cos(\nu\varphi) - B_\nu^\pm \sin(\nu\varphi)] \quad (2)$$

$$H_\varphi^\pm(\rho, \varphi) = \frac{\mp j}{\omega\mu} \frac{\partial}{\partial \rho} [J_\nu(\pm k\rho)][A_\nu^\pm \sin(\nu\varphi) + B_\nu^\pm \cos(\nu\varphi)] \quad (3)$$

$$H_z^\pm(\rho, \varphi) = 0 \quad (4)$$

Imposition of the boundary conditions across the faces of the wedge separating the DPS and DNG regions, *i.e.* the continuity of  $E_z$  and  $H_\rho$  across the interfaces, leads to an algebraic system of four homogenous equations for the four unknowns integration constants  $A_\nu^\pm$  and  $B_\nu^\pm$ ; for nonzero fields to exist, the determinant of the coefficients must be zero, yielding:

$$\sin((\pi - 2\alpha)\nu) = 0 \quad (5)$$

The resonance condition (5) determines the possible values of the separation constant  $\nu$ . If  $\alpha \neq \pi/2$ , the condition (5) leads to the discrete set of values:

$$\nu_m = \frac{m\pi}{\pi - 2\alpha}, \quad (m = 0, \pm 1, \pm 2, \dots) \quad (6)$$

in particular, if the resonator is completely filled with only one material ( $\alpha = 0$  or  $\pi$ ), then  $\nu_m$  is an integer, as expected. The boundary condition, that the tangent electric field be zero on the metallic walls of the resonator, yields:

$$J_{\nu_m}(ka) = 0 \quad (7)$$

from which the resonator frequencies are derived. Hence, if  $\alpha \neq \pi/2$ , phase compensation between DPS and DNG subvolumes cannot occur. However, if  $\alpha = \pi/2$ , *i.e.* if the DPS and DNG sub-volumes are semi-cylinders of equal size, then the resonance condition (5) is identically satisfied, and the boundary condition on the PEC walls

$$J_\nu(ka) = 0 \quad (8)$$

yields the allowed values of  $\nu$  for any preassigned frequency: phase compensation always occurs, and the cylinder resonates at all frequencies for which the DNG material behaves as postulated.

### III. SOLUTION FOR LINE SOURCE EXCITATION

Let us consider an electric line source  $\mathbf{J}$  parallel to  $z$  axis and located at  $(\rho_o, \varphi_o)$  inside the DPS sub-volume (see Fig. 1):

$$\mathbf{J} = J_z \hat{z} = I_o \frac{1}{\rho_o} \delta(\rho - \rho_o) \delta(\varphi - \varphi_o) \hat{z} \quad (9)$$

where  $I_o$  is the intensity (in A) and  $\delta$  is the delta function.

The longitudinal component  $E_z$  of the electric field must satisfy the following equation:

$$\left( \frac{\partial^2}{\partial \rho^2} + \frac{1}{\rho} \frac{\partial}{\partial \rho} + \frac{1}{\rho^2} \frac{\partial^2}{\partial \varphi^2} + k^2 \right) E_z(\rho, \varphi) = -j\omega\mu_o J_z \quad (10)$$

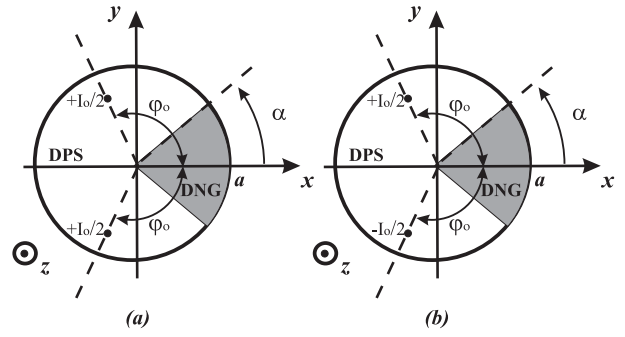


Fig. 2. Cross section of the two symmetries

with boundary conditions at the DPS/DNG interface and at the cylindrical border.

The solution of the problem is found by employing the resolvent technique [10]. This technique requires the evaluation of the one dimensional characteristic Green function in the azimuthal direction. In order to reduce this problem to the solution of a Sturm-Liouville (SL) problem on a finite interval, we need to consider the azimuthal periodicity of the field  $E_z$ . For the presence of the DNG sector we cannot resort to the expedient used in [10] Ch.3.4b for the resonator filled by a homogeneous DPS medium.

However, since (10) is linear, the solution of the problem shown in Fig. 1 may be obtained by superposition of the solutions of the two problems shown in Fig. 2, that involve symmetric (Fig. 2a) and anti-symmetric (Fig. 2b) line sources with respect to the plane  $y = 0$ . These two configurations are equivalent to inserting a perfect magnetic conductor (PMC) in the plane  $y = 0$  of Fig. 2a, and a perfect electric conductor (PEC) in the plane  $y = 0$  of Fig. 2b. In this way, we are facing the solution of two SL problems defined on finite intervals using the additional PMC and PEC boundary conditions. This can be accomplished by resorting to azimuthal non-uniform transmission lines (see Appendix I).

Let us indicate with  $E_z^{(1)}(\rho, \varphi)$  and  $E_z^{(2)}(\rho, \varphi)$  the electric fields that are present inside the cavities of Fig. 2a and Fig. 2b, respectively. Then the electric field inside the resonator of Fig. 1 is

$$E_z(\rho, \varphi) = E_z^{(1)}(\rho, \varphi) + E_z^{(2)}(\rho, \varphi) \quad (11)$$

The fields  $E_z^{(\ell)}(\rho, \varphi)$  ( $\ell = 1, 2$ ) of (11) are found employing a Green resolvent technique [10]. It yields:

$$E_z^{(\ell)}(\rho, \varphi) = -j\omega\mu_o I_o \sum_{n=0}^{\infty} \sum_{m=0}^{\infty} w(\varphi_o) \frac{\Phi^{(\ell)*}(\rho_o, \varphi_o) \Phi^{(\ell)}(\rho, \varphi)}{k^2 - k_{mn}^2} \quad (12)$$

where  $w(\varphi_o) = -1 + 2u(\varphi_o - \alpha)$ ,  $u$  is the unit step function, the asterisk indicates the complex conjugate,  $k_{mn}a$  is the  $n^{\text{th}}$  zero of (7),

$$\Phi^{(1)}(\rho, \varphi) = \frac{\sqrt{2}J_{\nu_m}(z_n(\nu_m)\rho/a)}{aJ_{\nu_m+1}(z_n(\nu_m))} \sqrt{\frac{\xi_m}{\pi-2\alpha}} \cdot [\cos(\nu_m\varphi)u_1(\varphi) + \cos(\nu_m(2\alpha-\varphi))u_o(\varphi)] \quad (13)$$

with  $\xi_m = 2$  except  $\xi_0 = 1$  and where  $u_1(\varphi) = u(\varphi) - u(\varphi - \alpha)$ ,  $u_o(\varphi) = u(\varphi - \alpha) - u(\varphi - \pi)$ . The function  $\Phi^{(2)}(\rho, \varphi)$  is obtained from  $\Phi^{(1)}(\rho, \varphi)$  by replacing the two cosine functions in (13) with sine functions of the same arguments.

The technique leading to the solution (12) fails when  $\alpha = \pi/2$ , because the characteristic Green function that relies on (6) cannot be defined. This peculiar case will be considered in future work.

TABLE I  
VALUES OF  $k_{mn}a$  FOR  $\alpha = 0$

m	$\nu_m$	$k_{m1}a$	$k_{m2}a$	$k_{m3}a$	$k_{m4}a$	$k_{m5}a$	$k_{m6}a$
0	0	2.405	5.520	8.654	11.792	14.931	18.071
1	1	3.832	7.016	10.173	13.324	16.471	19.616
2	2	5.136	8.417	11.620	14.796	17.960	21.117
3	3	6.380	9.761	13.015	16.223	19.409	22.583
4	4	7.588	11.065	14.373	17.616	20.827	24.019
5	5	8.771	12.339	15.700	18.980	22.218	25.430
6	6	9.936	13.589	17.004	20.321	23.586	26.820
7	7	11.086	14.821	18.288	21.642	24.935	28.191
8	8	12.225	16.038	19.555	22.945	26.267	29.546
9	9	13.354	17.241	20.807	24.234	27.584	30.885
10	10	14.476	18.433	22.047	25.509	28.887	32.212
11	11	15.590	19.616	23.276	26.773	30.179	33.526

TABLE II  
VALUES OF  $k_{mn}a$  FOR  $\alpha = \pi/7$

m	$\nu_m$	$k_{m1}a$	$k_{m2}a$	$k_{m3}a$	$k_{m4}a$	$k_{m5}a$	$k_{m6}a$
0	0	2.405	5.520	8.654	11.792	14.931	18.071
1	7/5	4.363	7.585	10.759	13.919	17.072	20.221
2	14/5	6.135	9.496	12.740	15.941	19.122	22.292
3	21/5	7.827	11.322	14.640	17.891	21.107	24.303
4	28/5	9.472	13.091	16.485	19.787	23.041	26.267
5	7	11.086	14.821	18.288	21.642	24.935	28.191
6	42/5	12.678	16.521	20.057	23.462	26.795	30.083
7	49/5	14.252	18.196	21.800	25.255	28.628	31.948
8	56/5	15.812	19.851	23.520	27.025	30.436	33.788
9	63/5	17.361	21.491	25.222	28.774	32.224	35.607
10	14	18.900	23.116	26.907	30.506	33.993	37.408
11	77/5	20.431	24.729	28.579	32.222	35.746	39.192

#### IV. NUMERICAL RESULTS

The first few roots  $k_{mn}a$  of (7) are listed in Table I for  $\alpha = 0$  (no DNG sector present), and in Table II for  $\alpha = \pi/7$ . As expected, the roots are the same in the two cases when  $m = 0$ ; when  $m > 0$ , the roots in Table II are larger than the corresponding roots in Table I.

As an example, we consider a line source of intensity  $I_o = 1A$  located at  $(\rho_o = 0.7a, \varphi_o = 5\pi/8)$  when  $\alpha = \pi/7$  and  $ka = 5$ . The amplitudes of the even field  $|E_z^{(1)}|$ , odd field  $|E_z^{(2)}|$ , and total field  $|E_z|$  obtained from (11)-(12) by truncating the infinite series to  $n_{max} = m_{max} = 10$  are shown in Fig. 3. The large field amplitude of Fig. 3c in the neighborhood of the source image with respect to the plane  $y = 0$  bisecting the DNG wedge, may be physically understood by considering the negative Snell refractions across the wedge surfaces of the rays emanating from the line source.

The relative error between the amplitudes of Fig. 3c and those obtained by extending the summations to  $n_{max} = m_{max} = 11$  is shown in Fig. 4. While it is difficult to establish a convergence criterion for the series (12), it would appear that reasonably accurate results are obtained by selecting  $n_{max} = m_{max} = 2ka$ .

A vector plot of the direction and intensity of the magnetic field associated to the electric field of Fig. 3c is shown in Fig.5.

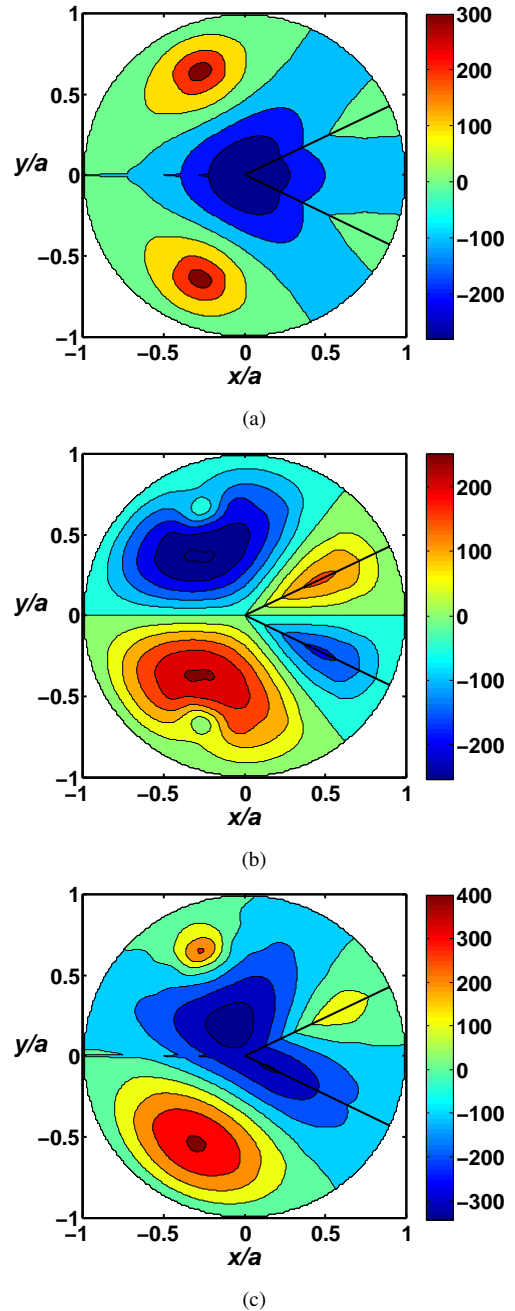


Fig. 3. Amplitudes (a)  $|E_z^{(1)}|$ , (b)  $|E_z^{(2)}|$ , and (c)  $|E_z|$  (in V/m) for  $I_o = 1A$ ,  $\rho_o = 0.7a$ ,  $\varphi_o = 5\pi/8$ ,  $\alpha = \pi/7$  and  $ka = 5$ , obtained from (11)-(12) with  $n_{max} = m_{max} = 10$ .

#### V. CONCLUSION

A metallic cylindrical resonator containing two lossless media anti-isorefractive to each other and separated by the faces of a wedge whose edge is located on the resonator axis has been studied, in the phasor domain. The conditions for resonances to exist have been found, the exact fields inside the resonator have been determined when the excitation is a line source parallel to the cylinder axis, and some numerical results have been displayed. It has been shown that resonances occur independently of the diameter of the resonator only when the faces of the wedge lie in the same plane, *i.e.* when the wedge has an aperture angle of  $\pi$  radians. This particular case will

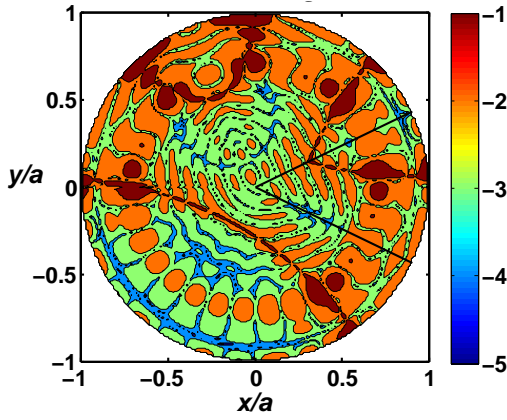


Fig. 4. Relative error (in  $\log_{10}$  scale) between  $|E_z|_{n_{max}=m_{max}=10}$  and  $|E_z|_{n_{max}=m_{max}=11}$ .

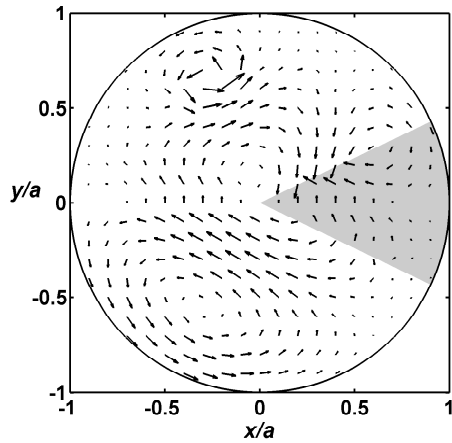


Fig. 5. Vector plot of the magnetic field associated to the electric field of Fig. 3c.

be examined in detail in a future work.

#### APPENDIX

##### NON-UNIFORM AZIMUTHAL TRANSMISSION LINE

Without loss of generality we refer to the PMC symmetry of Fig. 2a. Using separation of variables in (10) we need to construct an orth-normal basis for the equation

$$\left( \frac{d^2}{d\varphi^2} + \nu^2 \right) F_\nu(\varphi) = 0 \quad (14)$$

with boundary conditions at the interface of the media, at the PEC cylindrical border and at the additional PMC interface. Problem (14) can be treated with (characteristic) resolvent technique. The characteristic Green function  $g(\varphi, \varphi', \lambda)$  of a Sturm-Liouville problem must satisfy the following equation:

$$\left( \frac{d}{d\varphi} p(\varphi) \frac{d}{d\varphi} + \lambda w(\varphi) \right) g(\varphi, \varphi', \lambda) = -\delta(\varphi, \varphi') \quad (15)$$

Note that  $\lambda$  is an arbitrary parameter and the functions  $p(\varphi)$  and  $w(\varphi)$  arise from the presence of non-homogeneous media. The application of (14) to our problem (15) yields the following definitions

$$p(\varphi) = w(\varphi) = -1, \quad \text{for } 0 < \varphi < \alpha, \quad (\text{DNG}) \quad (16)$$

$$p(\varphi) = w(\varphi) = +1, \quad \text{for } \alpha < \varphi < \pi, \quad (\text{DPS}) \quad (17)$$

and boundary conditions

$$\frac{\partial g(\varphi, \varphi', \lambda)}{\partial \varphi} \Big|_{\varphi=\pi} = \frac{\partial g(\varphi, \varphi', \lambda)}{\partial \varphi} \Big|_{\varphi=0} = 0. \quad (18)$$

To solve equations (15), it is useful to define the circuit model of the problem using a non-uniform transmission line [10] as shown in Fig. 6. For  $0 < \varphi < \alpha$  (DNG medium) we have

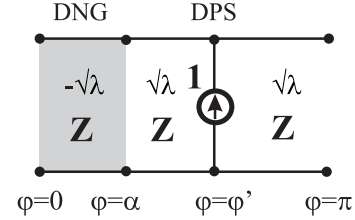


Fig. 6. Non-uniform transmission line equivalent to the problem (15) with conditions (16)-(18): PMC symmetry.

a transmission line with propagation constant  $\nu(\varphi) = -\sqrt{\lambda}$  and characteristic impedance  $Z$ . Conversely, for  $\alpha < \varphi < \pi$  (DPS medium) we have a transmission line with propagation constant  $\nu(\varphi) = +\sqrt{\lambda}$  and characteristic impedance  $Z$ . Note that, condition (18) results in open circuits at  $\varphi = 0, \pi$ . The method for the construction of  $g(\varphi, \varphi', \lambda)$  is reported in chapter 3.3 of [10] and is based on the knowledge of the solution of the transmission line problem.

#### ACKNOWLEDGMENT

This research was supported in part by the Italian Ministry of Education, University and Research (MIUR) under PRIN grant 20097JM7YR.

#### REFERENCES

- [1] N. Engheta, "Compact cavity resonators using metamaterials with negative permittivity and permeability," *Proc. Intl. Conf. Electromagnetics in Advanced Applications (ICEAA'01)*, Torino, Italy, Sept. 2001, pp. 739–742.
- [2] N. Engheta, "An idea for thin subwavelength cavity resonators using metamaterials with negative permittivity and permeability," *IEEE Antennas Wireless Propag. Lett.*, vol. 1, pp. 10–13, 2002.
- [3] S. Couture, A. Parsa and C. Caloz, "Design of a size-independent zero-permittivity rectangular resonator and possible antenna applications," *14th Intl. Symposium on Antenna Technology and Applied Electromagnetics (ANTEM)*, Ottawa, Canada, July 2010, pp. 1–4.
- [4] S. Couture, A. Parsa and C. Caloz, "Size-independent zeroth-order electric plasmonic cavity resonator," *Microwave Opt. Tech. Lett.*, vol. 53, pp. 927–932, April 2011.
- [5] P.L.E. Uslenghi, "A miniaturized parallelepipedal cavity resonator," *IEEE Antennas and Wireless Propag. Lett.*, vol. 9, pp. 807–808, 2010.
- [6] P.L.E. Uslenghi, "Size-Independent Prism Resonator Partially Filled With DNG Metamaterial," *IEEE Antennas Wireless Propag. Lett.*, vol. 10, pp. 746–747, 2011.
- [7] P.L.E. Uslenghi, "Size-independent metamaterial resonators," *EuCAP 2011*, Rome, Italy, Ap. 2011.
- [8] V.G. Daniele, R. D. Graglia, G. Lombardi and P. L. E. Uslenghi, "Cylindrical resonators partially filled with DNG metamaterial," *IEEE Intl. Symp. Antennas Propag. and URSI Meeting*, Spokane, WA, July 2011.
- [9] V.G. Daniele, R. D. Graglia, G. Lombardi and P. L. E. Uslenghi, "Cylindrical resonator sectorially filled with DNG metamaterial and excited by a line source," *USNC-URSI National Radio Science Meeting*, Boulder, CO, USA, Jan. 2012.
- [10] L.B. Felsen and N. Marcuvitz, *Radiation and Scattering of Waves*. New York: IEEE Press, 1994.